ORIGINAL

Visualization of cardiac dipole using a current density map : detection of cardiac current undetectable by electrocardiography using magnetocardiography

Hiroyuki Ikefuji, Masahiro Nomura*, Yutaka Nakaya**, Toshifumi Mori***, Noriyasu Kondo***, Kiyoshi Ieishi***, Sayuri Fujimoto***, and Susumu Ito***

*Department of Cardiology, JA Kochi Hospital, Kochi, Japan, *Faculty of Integrated Art and Sciences, Department of Human and Social Sciences, The University of Tokushima, **Department of Nutrition and Metabolism, and ***Department of Digestive and Cardiovascular Medicine, Institute of Health Biosciences, The University of Tokushima Graduate School, Tokushima, Japan*

Abstract : A close relationship exists between electric current and the magnetic field. However, electricity and magnetism have different physical characteristics, and magnetocardiography (MCG) may provide information on cardiac current that is difficult to obtain by electrocardiography (ECG). In the present study, we investigated the issue of whether the current density map method, in which cardiac current is estimated from the magnetic gradient, facilitates the visualization of cardiac current undetectable by ECG.

The subjects were 50 healthy adults (N group), 40 patients with left ventricular overloading (LVO group), 15 patients with right ventricular overloading (RVO group), 10 patients with an old inferior myocardial infarction (OMI group), and 30 patients with diabetes mellitus (DM group). MCGs were recorded with a second derivative superconducting quantum interference device (SQUID) gradiometer using liquid helium. Isopotential maps and current density maps from unipolar precordial ECG leads and MCGs, respectively, were prepared, and the cardiac electric current was examined.

The current density map at the ventricular depolarization phase showed one peak of current density in the N group. However, in the OMI group, the current density map showed multiple peaks of current density areas. In the RVO group, two peaks of current densities were detected at the right superior region and left thoracic region and these two diploles appeared to be from the right and left ventricular derived cardiac currents, respectively. Moreover, there was a significant correlation between the magnitude of the current density from the right ventricle and the systolic pulmonary arterial pressure. The current density map at the ventricular repolarization phase in the N group showed only a single current source. However, abnormal current sources in the current density maps were frequently detected even in patients showing no abnormalities on isopotential maps in the LVO, DM, and OMI groups.

The findings herein suggest that opposing dipoles of the ventricular depolarization and repolarization vectors were summed and evaluated as a single dipole in the electrocardiogram. However, MCG facilitated the detection of multiple dipoles because of its superior spatial resolution as well as difference in physical properties between magnetic and electrical fields. Our results suggest that MCG with a current density map is useful for detecting cardiac current undetectable by ECG in an early stage. J. Med. Invest. 54 : 116-123, February, 2007

Keywords **:** *magnetocardiography, current density map, cardiac current*

Received for publication November 21, 2006 ; accepted December 28, 2006.

Address correspondence and reprint requests to Masahiro Nomura, M.D., Ph.D., Faculty of Integrated Art and Sciences, The University of Tokushima, Minami-Jyosanjima, Tokushima 770-8502, Japan and Fax : +81-88-656-6173.

INTRODUCTION

The electrical current from the heart has a magnetic field component, and magnetocardiograms reflect the heart-derived magnetic field. This magnetic field is extremely weak, and corresponds to 1/1,000,000 of the geomagnetism. Therefore, a superconducting quantum interference device (SQUID) magnetocardiometer must be used in order to detect it (1, 2).

A close relationship exists between the electric current and the magnetic field. However, electricity and magnetism have different physical characteristics, and magnetocardiography (MCG) may provide information on cardiac current that is difficult to obtain by electrocardiography (ECG) (3). Although a magnetic isofield map can be used to express magnetic field resulting from cardiac current for many years, cardiac current is estimated according to Bio Sabar's laws (4). Therefore, untrained physician cannot have the direct idea of current dipole from this map.

In the present study, the issue of whether the current density map method, in which cardiac current can be estimated from the magnetic gradient would facilitate the visualization of cardiac current undetectable by ECG was investigated.

SUBJECTS AND METHODS

1) Subjects

The subjects were 50 healthy adults (N group : 40 men, 10 women, 45.2±13.6 years), 40 patients with left ventricular overloading (LVO group : 30 men, 10 women, 52.9±12.8 years), 15 patients with right ventricular overloading (RVO group : 7 men, 8 women, 42.2±15.6 years), 25 patients with old inferior myocardial infarction (OMI group : 14 men, 11 women, 58.9±10.2 years) and 30 patients with diabetes mellitus (DM group : 13 men, 17 women, 52.2±12.6 years).

The N group consisted of 50 healthy adults in whom physical findings were normal without a history of heart or respiratory disease, a resting blood pressure of 140/90 mmHg or less, and no abnormalities on standard 12-lead ECG, chest X-ray, urinalysis, or blood biochemistry.

The LVO group consisted of 40 patients with essential hypertension in whom the resting blood pressure was 160/90 mmHg or more. Patients with myocardial infarctions, valvular heart disease, or diabetes were excluded from the study. The RVO group consisted of 4 patients with atrial septal defects, 1 patient with pulmonary arterial stenosis, 6 patients with mitral valve stenosis, 2 patients with pulmonary vascular disease, and 2 patients with primary pulmonary hypertension in whom these disorders were diagnosed based on physical, echocardiography, chest X-ray, and standard 12-lead ECG findings. Pulmonary arterial pressure was measured on right cardiac catheterization in all patients of the RVO the group.

Old inferior myocardial infarction was diagnosed based on the patient's medical history, laboratory data such as abnormal serum myocardial enzyme levels, and echocardiography and ECG findings. All patients in the OMI group were examined more than 2 months after the acute myocardial infarction attack. The patients of the DM group were diagnosed according to the criteria for a 75 g glucose tolerance test. Patients in whom standard 12-lead ECGs showed abnormal Q waves and those with heart disease such as valvular heart disease and cardiomyopathy were excluded from the study.

In all groups, subjects with ventricular conduction disorders such as complete right or left bundle branch block and pre-excitation syndrome were excluded. Prior to participation in the present study, written informed consent was obtained from all subjects.

2) Magnetocardiography and unipolar lead electrocardiography

A second derivative SQUID magnetocardiometer using liquid helium was employed for the MCG. The subjects were laid in a supine position on a nonmagnetic bed, and a magnetic detector was placed close to the thoracic wall and the magnetic component perpendicular to the chest wall was recorded simultaneously with the lead II ECG. The points for recording the MCG are shown in Fig. 1. The vertical lines passed through C_{3R} to C_4 of the ECG and the mid point between C_4 and C_5 of the ECG. These lines were designated 0, 1, 2, 3, 4, 4', respectively. There were six horizontal lines ; namely, the first to sixth intercostals lines, designated A, B, C, D, E and F, respectively. The MCGs were recorded at the intersections of these lines. The sensitivity of the MCG was controlled at 1.05×10^{-11} tesla/cm.

3) Current density map and isopotential map

At the 36 leads in the anterior thoracic region, current dipoles were calculated from the magnetic gradients for 2 points adjacent to each other. Regard-

ing the lead II ECG as the time reference, spline complementation for current distribution in the anterior thoracic region from magnetic fields at the 36 leads were performed, and a current density map was constructed.

The current-arrow maps were calculated from the derivatives of the normal component (Bz) of the MCG signals as Ix=dBz/dy and Ix=dBz/dy. Where Ix and Iy are magnitude of current arrow in X and Y directions, respectively. Current density map method displays a contour map of the current density. The magnitude of current density (CD) at each position was calculated as follows (4-6). CD= $(Ix^2+Iy^2)^{1/2}$

Furthermore, an isopotential map from unipolar lead ECGs recorded at the 36 leads were prepared, regarding lead II ECGs as the time reference.

4) Statistical analysis

Statistical analyses were performed using a PC computer. Comparisons between the two groups were performed using chi-square test. Statistical significance was set at $p<0.05$.

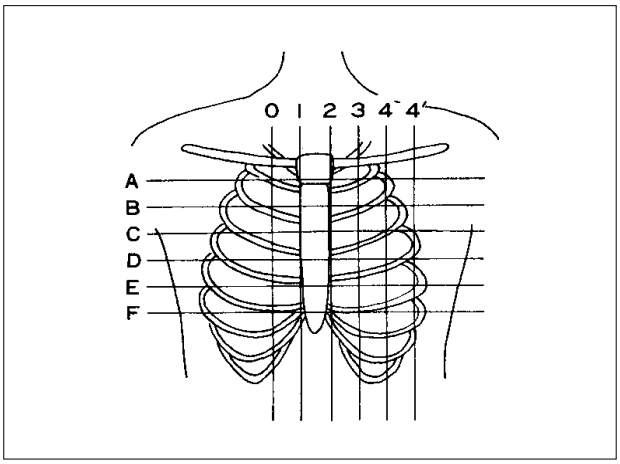

Fig. 1 Points for recording the MCG.

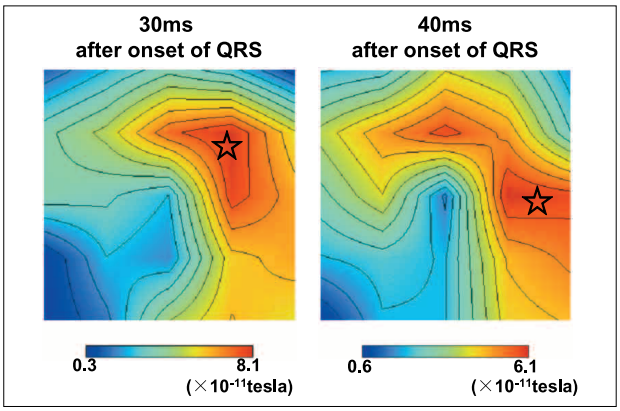

Fig. 2 Current density maps at 30 and 40 msec after the onset of the QRS wave in a healthy adult. ☆ : peak of current density.

RESULTS

1) Current density maps in ventricular depolarization vectors

(1) Ventricular depolarization vectors in healthy adults (N) group

Fig. 2 shows current density maps at 30 and 40 msec after the onset of the QRS wave in a healthy adult. A single peak of current density was noted on these maps. In the N group, current density maps at 30 to 40 msec after the onset of the QRS wave showed a single current density peak for all subjects. No subject showed 2 or more peak of current density.

(2) Ventricular depolarization vectors in patients with old myocardial infarction (OMI) group

Fig. 3 shows isopotential and current density maps at 30 and 40 msec after the onset of the QRS wave in a patient with an old inferior myocardial infarction. On the isopotential map at 30 and 40 msec after the onset of the QRS wave, a minimum was noted at the center of the anterior thorax, and a maximum was noted in the left superior anterior thoracic region, suggesting a single dipole in the left superior direction. However, the current density map in this patient showed two peaks of current densities, one at the center of the anterior thorax and the other on the left.

Fig. 4 shows isopotential and current density maps at 30 and 40 msec after the onset of the QRS wave in another patient with an old inferior myocardial infarction. On the isopotential map at 30 and 40 msec after the onset of QRS wave, a minimum was noted in the superior anterior thoracic region, and a maximum was noted in the left inferior anterior thoracic region, suggesting a single dipole in the left inferior direction. However, the current density map in this patient showed two peaks of current densities, one

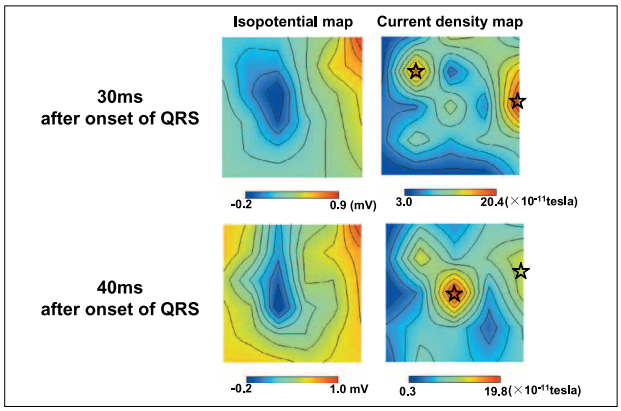

Fig. 3 Isopotential and current density maps at 30 and 40 msec after the onset of the QRS wave in a patient with an old inferior myocardial infarction. ☆ : peak of current density.

at the center of the anterior thorax and the other on the left.

In the OMI group, current density maps 30 to 40 msec after the onset of QRS wave showed two peaks of current densities, different from those in the N group. In the OMI group, the presence of multiple current sources was suggested in 4 patients, with the absence of multiple current sources on the isopotential map. Multiple current sources were significantly detected in current density maps than isopotential maps ($p<0.01$).

(3) Ventricular depolarization vectors in the patients with right ventricular overloading (RVO) group

Fig. 5a and 5b show current density maps at 60 msec after the onset of the QRS wave in a healthy adult and a patient with right ventricular overloading, respectively. A single peak of current density (current density = 8.1×10^{-11} tesla) was noted at the left center of the anterior thorax in Fig. 5a. On the other hand, in a patient with right ventricular overloading, as shown in Fig. 5b, a cardiac current (current density = 21.6×10^{-11} tesla) was separately observed in the right superior region in addition to the current source (current density = 7.9×10^{-11} tesla) at the left center of the anterior thorax.

Fig. 6 shows the correlation between the current density at the right superior region and systolic pulmonary arterial pressure in the RVO group. There was a significant correlation between systolic pulmonary arterial pressure and the estimated magnitude of current density from the right ventricle ($r=+0.73$, $p<0.01$).

2) Current density maps in ventricular repolarization vectors

(1) Ventricular repolarization vectors in healthy adults

Fig. 7 shows isopotential and current density maps in the peak of the T wave on a lead II ECG in a healthy adult. On the isopotential map in the ventricular repolarization phase, a negative area was detected in the right superior direction, and a maximum was noted at the left center of the anterior

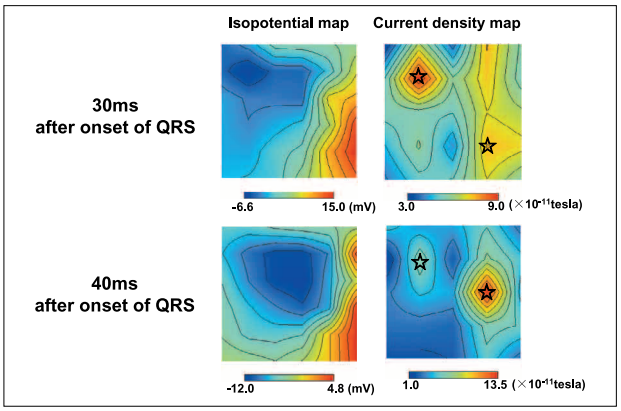

Fig. 4 Isopotential and current density maps at 30 and 40 msec after the onset of the QRS wave in another patient with an old inferior myocardial infarction. ☆ : peak of current density.

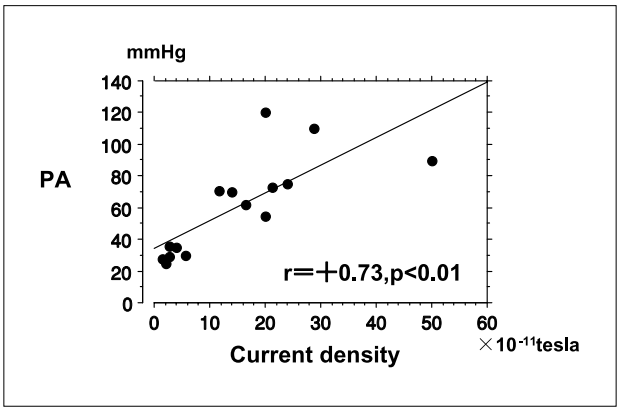

Fig. 6 Correlation between the estimated magnitude of current density and systolic pulmonary arterial pressure in the RVO group. PA, systolic pulmonary arterial pressure (mmHg).

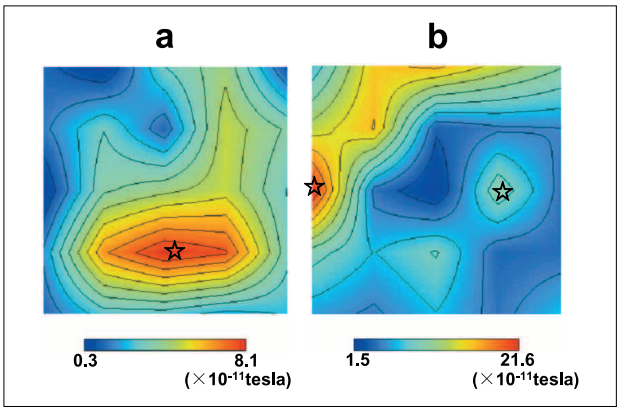

Fig. 5 Current density maps at 60 msec after the onset of the QRS wave. (Panel a, healthy adult ; Panel b, patient with right ventricular overloading.) ☆ : peak of current density.

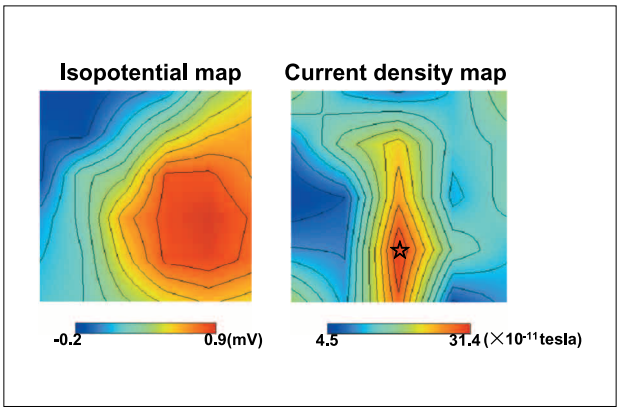

Fig. 7 Isopotential and current density maps in the peak of the T wave on a lead II ECG in a healthy adult. ☆ : peak of current density.

thorax, suggesting a single dipole toward the left inferior. On the current density map, a single current source was also noted at the left center region of the anterior thorax. In the N group, a single peak of current density was observed in all subjects, and none showed multiple peaks of current densities.

(2) Ventricular repolarization vectors in the left ventricular overloading (LVO) group

Fig. 8a shows isopotential and current density maps in the peak phase of the T wave on a lead II ECG for a patient with essential hypertension. On the isopotential map of this patient, a negative area was detected in the right superior direction, and a maximum was noted at the left center of the anterior thorax, suggesting a single dipole toward the left inferior. The pattern of the isopotential map was similar to that in the healthy adult shown in Fig. 7. However, on the current density map, two peaks of current densities were noted at the left center of the anterior thorax and in the inferior area, suggesting the presence of two peaks of current sources.

Fig. 8b shows isopotential and current density maps in the peak phase of the T wave on a lead II ECG for a patient with severe essential hypertension. On the isopotential map of this patient, a minimum was detected in the left anterior thoracic region, and a maximum was noted at the center of the anterior thorax, suggesting a single dipole toward the right. On the other hand, on the current density map, two peaks of current densities were noted, one at the left center of the anterior thorax and the other in the right inferior area, suggesting the presence of two peaks of current sources.

In the LVO group, two current sources were present on current density maps in 37.5% of the patients who showed normal findings on body surface ECG. Two current sources were present on the current density maps in 60.0% of patients with a dipole toward the right on the isopotential map, as shown in Fig. 8b. Multiple current sources were significantly detected in current density maps than isopotential maps ($p<0.001$).

(3) Ventricular repolarization vectors in the diabetes mellitus (DM) group

Fig. 9 shows isopotential and current density maps in the peak of the T wave on a lead II ECG for a patient with diabetes. On the isopotential map of this patient, a negative area was detected in the right superior direction, and a maximum was noted at the left center of the anterior thorax, suggesting a single dipole toward the left inferior. The pattern of the isopotential map was similar to that for the healthy adult shown in Fig. 7. However, on the current density map, two maxima were noted, one at the left center of the anterior thorax and the other in the inferior area, suggesting the presence of two current sources.

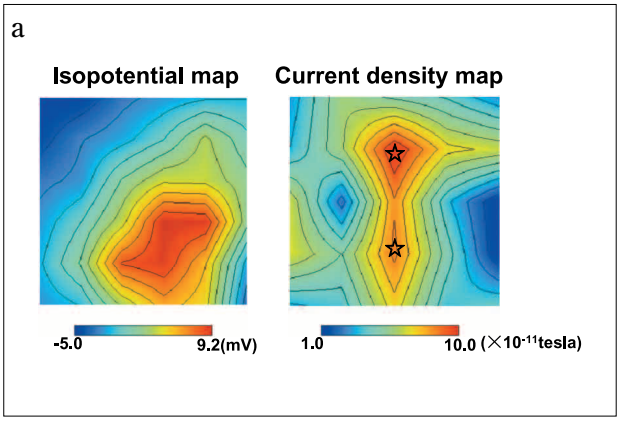

Fig. 8 Isopotential and current density maps in the peak phase of the T wave. (Panel a, patient with mild essential hypertension ; Panel b, patient with severe essential hypertension) ☆ : peak of current density.

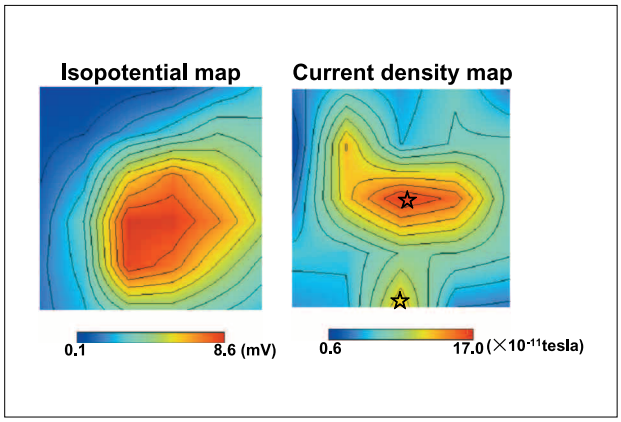

Fig. 9 Isopotential and current density maps in the peak of the T wave on a lead II ECG for a patient with diabetes. ☆ : peak of current density.

In the DM group, the current density maps suggested the presence of two current sources in 33.3% of the patients without abnormalities on a body surface ECG. Two current densities were significantly detected in current density maps than body surface ECGs ($p<0.01$).

(4) Ventricular repolarization vectors in the OMI group

Fig. 10 shows isopotential and current density maps in the of the T wave on a lead II ECG for a patient with an old inferior myocardial infarction. On the isopotential map of this patient, a negative area was detected in the right superior direction, and a maximum was noted at the left center of the anterior thorax, suggesting a single dipole toward the left inferior. The pattern of the isopotential map was similar to that for the healthy adult shown in Fig. 7. However, on the current density map, two maxima were noted, one at the center of the anterior thorax and the other in the right inferior area, suggesting the presence of two current sources. On current density maps, current dipoles, which could not be detected as abnormalities on a body surface ECG, as demonstrated in this patient, were detected as abnormal current sources in 36.0% of the OMI group. Abnormal current dipoles were significantly detected in current density maps than body surface ECGs ($p<0.001$)

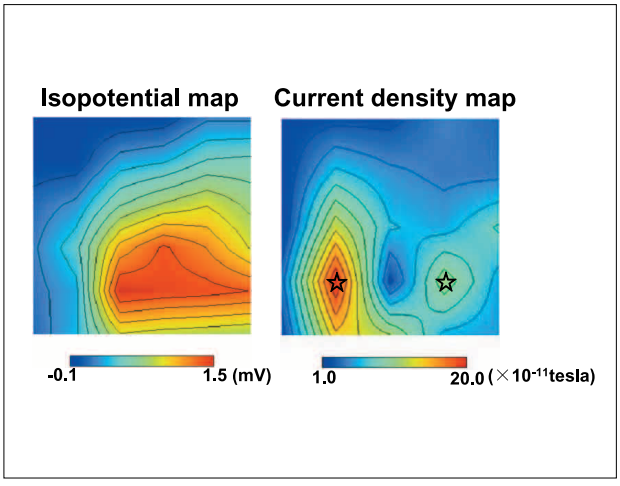

Fig. 10 Isopotential and current density maps in the of the T wave on a lead II ECG for a patient with an old inferior myocardial infarction. ☆ : peak of current density.

DISCUSSION

There have been several methods for expressing cardiac current dipole, a magnetic isofield map, a vector arrow map, and so on. In the present study, expressing the cardiac magnetic field using a current density map facilitated the detection of ventricular depolarization and repolarization vectors undetectable by ECG, suggesting its clinical usefulness.

1. Ventricular depolarization vectors and the current density map

(1) Ventricular depolarization vectors in patients with old myocardial infarction

The ECG findings for the patient with small myocardial necrosis is expressed as a non-Q wave myocardial infarction or subendocardial infarction and an abnormal Q wave, expressing myocardial necrosis (7-9), could not be detected by an ECG in this patient. When the residual normal myocardium accounts for more than 30% of the myocardium, motion abnormalities can not be detected using echocardiography or left ventriculography, but abnormal cardiac currents could be detected by the MCG method, even in these patients (7-9). As shown in Fig. 4, two separate current sources derived from the normal myocardium and a necrotic myocardial lesion could be detected on the current density map even in the patient with only a single dipole in the left inferior direction on the isopotential map.

(2) Ventricular depolarization vectors in patients with right ventricular overloading

The ECG diagnosis of right ventricular overloading is not highly accurate (10-12). However, since the distance between right ventricular current and a magnetic sensor is short, a current dipole itself can be detected more easily by the MCG, thus improving the accuracy of the diagnosis (13, 14). In the MCG, the right ventricle is located in an area adjacent to a magnetic sensor, and this procedure is more advantageous than ECG for evaluating cardiac current from the right ventricular magnetic field. This may contribute to the greater accuracy in an MCG diagnosis of right ventricular overloading (13, 14). Moreover, in this study, we investigated the ventricular depolarization abnormality of the RVO group at 60msec from the onset of QRS wave, because this phase is to reflect right ventricular muscle mass.

As shown in Fig. 5, the right ventricle derived current was observed separately, in addition to the left ventricular depolarization current in a patient with a right ventricular overloading. The present study suggests that pulmonary arterial pressure can

be non-invasively estimated by detecting the right ventricular current.

2. Ventricular repolarization vectors and the current density map

(1) Ventricular repolarization vectors in patients with left ventricular overloading

The current density map method may facilitate the early detection of cardiac current undetectable by an isopotential map (15). Moreover, the current density map may facilitate the simultaneous detection of normal and abnormal repolarization vectors (16). The pervious reports (15, 16) of ventricular repolarization were studied on a peak of T wave, and this study was also performed in a same phase.

Nomura, *et al.* (15) reported, using magnetic isofield and departure maps, that abnormal ventricular repolarization vectors were detected in 10.0% of patients with left ventricular overloading. In the present study, abnormal current sources were detected by the current density map method in 37.5% of patients without any abnormalities in the isopotential map. The above results suggest that the current density map method is more useful than the conventional MCG method for detecting abnormal current sources.

(2) Ventricular repolarization vectors in the DM group

It is known that diabetes frequently leads to the development of microvascular disorders (150 μm or less), leading to diabetic cardiomyopathy (18). In the present study, MCG facilitated the detection of the current source that could not be detected as an abnormality in the isopotential map (15, 16). In patients in whom abnormal current is detected in an early stage, strict diabetes control and early treatment for secondary cardiomyopathy might improve their prognosis.

(3) Ventricular repolarization vectors in the OMI group

Repolarization waves in the presence of a myocardial infarction serially normalize (19, 20). In the present study, two current sources were present in the current density map, even in infarction patients without abnormalities of ECG. Therefore, the current density map may be useful for evaluating residual myocardial ischemia. MCG facilitated the detection of an ischemia vector that was not detected by ECG, suggesting its clinical usefulness.

3. Current density map and its clinical usefulness

In the present examination of ventricular depolarization and repolarization vectors, multiple opposing dipoles were detected separately using a current density map as a single dipole in the method of ECG. In 1963, Baule and McFee (21) recorded a cardiac magnetic field for the first time. Since then, biomagnetism has been measured with a single-channel or multi-channel SQUID (22, 23). However, this procedure is not commonly applied due to the complexity and high cost of the instrumentation (3). ECG, which is routinely employed in clinical practice, is inexpensive and simple, and therefore, essential for clinical medicine.

However, recent studies have reported the usefulness of a magnetocardiograph (24-27). Along with the development of multi-channel devices, they are costly, making their widespread clinical use difficult. The present study suggests that a single channel magnetocardiograph facilitates the detection of abnormal cardiogenic currents on measurements at several points without the need for many leads. In conclusions, MCG with a current density map may be useful for predicting pulmonary arterial pressure in patients with right ventricular overloading, and for detecting cardiac current undetectable by electrocardiography, in an early stage.

REFERENCES

1. Zimmerman JE, Frederick NV : Miniature ultrasensitive superconducting magnetic gradiometer and its use in cardiography and other applications. Appl Phys Lett 19 : 16-19, 1971
2. Cohen D, Edelsack A, Zimmerman JE : Manetocardiograms taken inside a shielded room with a superconducting point-contact magnetometer. Appl Physics Letters 16 : 278-280, 1970
3. Mori H, Nakaya Y : Present status of clinical magnetocardiography. CV World Report 1 : 78-86, 1988
4. Nakaya Y, Sumi M, Saito K, Fujino K, Murakami M, Mori H : Analysis of current source of the heart using isomagnetic and vector arrow maps. Jpn Heart J 25 : 701-711, 1984
5. Kandori A, Kanzaki H, Miyatake K, Hashimoto S, Itoh S, Tanaka N, Miyashita T, Tsukada K : A method for detecting myocardial abnormality by using a current-ratio map calculated from an exercise-induced magnetocardiogram. Med

Biol Eng Comput 39 : 29-34, 2001
6. Hosaka H, Cohen D : Part IV : visual determination of generators of the magnetocardiogram. J Electrocardiol 9 : 426-432, 1976
7. Davidoff R, Goldman AP, Diamond TH, Smith R, Cilliers AJ, Myburgh DP : The natural history of the Q wave in inferoposterior myocardial infarction. S Afr Med J 61 : 611-612, 1982
8. Kalbfleisch JM, Shadaksharappa KS, Conrad LL, Sarkar NK : Disappearance of the Q-deflection following myocardial infarction. Am Heart J 76 : 193-198, 1968
9. Montague TJ, Johnstone DE, Spencer CA, Lalonde LD, Gardner MJ, O'Reilly MG, Horacek BM : Non-Q-wave acute myocardial infarction : body surface potential map and ventriculographic patterns. Am J Cardiol 58 : 1173-1180, 1986
10. Sokolow M, Lyon TP : The ventricular complex in right ventricular hypertrophy as obtained by unipolar precordial and limb leads. Am Heart J 38 : 273-294, 1949
11. Allenstein BJ, Mori H : Evaluation of electrocardiographic diagnosis of ventricular hypertrophy based on autopsy comparison. Circulation 21 : 401-412, 1960
12. Myers GB, Klein HA, Stofer BE : The electrocardiographic diagnosis of the right ventricular hypertrophy. Am Heart J 35 : 1-40, 1948
13. Fukuda Y, Sumi M, Nakaya Y : The magnetocardiogram in right ventricular overloading. Tokushima J Exp Med 34 : 83-90, 1987
14. Fukuda Y, Sumi M, Nakaya Y : Magnetocardiographic diagnosis of right ventricular overloading in mitral stenosis. Tokushima J Exp Med 34 : 91-96, 1987
15. Nomura M, Fujino K, Katayama M, Takeuchi A, Fukuda Y, Sumi M, Murakami M, Nakaya Y, Mori H : Analysis of the T wave of the magnetocardiogram in patients with essential hypertension by means of isomagnetic and vector arrow maps. J Electrocardiol 21 : 174-182, 1988
16. Nakaya Y, Nomura M, Fujino K, Ishihara S, Mori H : The T wave abnormality in the magnetocardiogram. Frontiers Med Biol Engng 1 : 183-192, 1989
17. Riff ER, Riff KM : Abnormalities of myocardial depolarization in overt, subclinical and prediabetes. A vectorcardiographic study. Diabetes 23 : 572-578, 1974
18. Seneviratne BI : Diabetic cardiomyopathy : the preclinical phase. Br Med J 1 : 1444-1446, 1977
19. Taccardi B : Body surface distribution of equipotential lines during atrial depolarization and ventricular repolarization. Cir Res 19 : 865-878, 1866
20. Nomura M, Nakaya Y, Fujino K, Ishihara S, Katayama M, Takeuchi A, Watanabe K, Hiasa Y, Aihara T, Mori H : Magnetocardiographic studies of ventricular repolarization in old inferior myocardial infarction. Eur Heart J 10 : 8-15, 1989
21. Baule MS, McFee R : Detection of the magneticfield of the heart. Am Heart J 66 : 95-97, 1963
22. Nomura M, Nakaya Y, Saito K, Kishi F, Wakatsuki T, Miyoshi H, Nishikado A, Bando S, Ito S, Nishitani H, Wada M, Fujita S, Tamura I : Noninvasive localization of accessory pathways by magnetocardiographic imaging. Clin Cardiol 17 : 239-244, 1994
23. Takeuchi A, Watanabe K, Nomura M, Ishihara S, Sumi M, Murakami M, Saito K, Nakaya Y, Mori H : The P wave in the magnetocardiogram. J Electrocardiol 21 : 161-167, 1988
24. Ogata K, Kandori A, Miyashita T, Tsukada K, Nakatani S, Shimizu W, Kanzaki H, Miyatake K, Yamada S, Watanabe S, Yamaguchi I : Visualization of three-dimensional cardiac electrical excitation using standard heart model and anterior and posterior magnetocardiogram. Int J Cardiovasc Imaging 22 : 581-593, 2006
25. Kim K, Lee YH, Kwon H, Kim JM, Bae JH : Independent component analysis for synthetic aperture magnetometry in magnetocardiography. Comput Biol Med 36 : 253-261, 2006
26. Fenici R : Construction of a three-dimensional outline of the heart and conduction pathway by means of a 64-channel magnetocardiogram in patients with atrial flutter and fibrillation. Int J Cardiovasc Imaging 21 : 563-564, 2005
27. Nakai K, Kawazoe K, Izumoto H, Tsuboi J, Oshima Y, Oka T, Yoshioka K, Shozushima M, Suwabe A, Itoh M, Kobayashi K, Shimizu T, Yoshizawa M : Construction of a three-dimensional outline of the heart and conduction pathway by means of a 64-channel magnetocardiogram in patients with atrial flutter and fibrillation. Int J Cardiovasc Imaging 21 : 555-561, 2005